EXTERNAL NOISE OF LIGHT PROPELLER-DRIVEN AIRCRAFT

F.W.J. van Deventer and G.J.J. Ruijgrok
Dept. of Aerospace Engineering
Delft University of Technology
Delft, The Netherlands.

Abstract

This paper describes an experimental research program set out to investigate basic sound characteristics of light propeller-driven airplanes and to quantify actual observed noise levels.
The method of data reduction makes it possible to calculate sound time-histories and peak noise levels at any point on the ground.
Some results are presented of systematic noise measurements during level and climbing flyovers of two types of light airplanes. Also the effect of variation of some operational parameters and of airframe drag reduction on observed noise levels is indicated.
Finally, measured data are compared with results of calculations, using a well-known emperical propeller noise prediction method. The need for improved prediction methods is stressed, since basic sound signatures show poor agreement.

I. Introduction

Noise problems not only are caused by military and large civil aircraft, the operations of small general aviation aircraft too are experienced as a nuisance in densely populated areas. To protect the public against unnecessary noise from small aircraft, a number of countries have published requirements concerning propeller-driven light aircraft noise certification[1,2].
All these regulations limit the maximum noise level, expressed in dB(A) and measured under the flight path during level flight at maximum continuous power at 300 m (1000 ft) altitude, as a function of gross weight. Data from these certification tests, however, give no information about actual noise levels observed in day-to-day operations, nor do they tell anything about the noise radiation signature. Neither they can be used to predict annoyance levels around airports, since annoyance is primarily caused during take-off and low level flying in the traffic pattern.

In order to investigate the external sound characteristics of light propeller-driven aircraft and to quantify the actual noise levels in several flight conditions, a test program has been developed at the Department of Aero-Space Engineering of Delft University of Technology. In this program, sound recordings are performed during level and climbing flights, together with the determination of the corresponding flight paths.
From these recordings the following basic sound source quantities are computed:

- The overall acoustic power radiated (expressed in power watt level, PWL)*.
- The distribution of overall power watt level over the frequency spectrum, in terms of 1/3-octave band frequencies (PWL(i)).
- The spatial distribution of the overall power watt level (expressed in overall Directivity Index , DI (θ), or overall sound pressure level, Lp (θ))*.
- The spatial distribution of power watt level in the different 1/3-octave band frequencies (Directivity Index, DI (θ,i)).
- The distribution of overall sound pressure level at given distance from the source over the frequency spectrum for a number of emission angles (Lp(θ,i)).

Besides the need to know these quantities for noise radiation analysis and for the computation of observed noise levels, they also provide a basis to check existing noise prediction methodologies and to adjust emperical constants in them as required.

As examples a few results of noise measurements are given for two single-engined propeller-driven aircraft having a gross weight of about 1000 kg

---

*Throughout this paper: PWL re 10^{-12} Watt and Lp re 2.10^{-5} N/m^2.

(2200 lb). General arrangements drawings of these aircraft are shown in Figure 1. They are equipped with the same four cylinder piston engine (Lycoming O-320, 150 rated horse power at 2700 RPM) and a two-bladed fixed pitch direct-drive propeller.

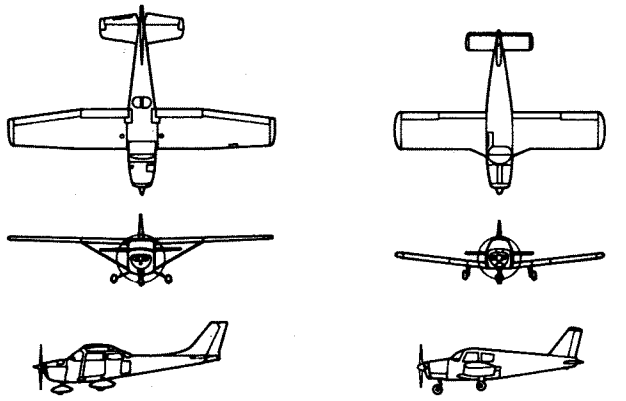

Cessna 172 Piper Cherokee PA-28

FIGURE 1. GENERAL ARRANGEMENTS OF TEST AIRCRAFT.

Within the category of light aircraft (maximum certificated take-off weight not exceeding 5700 kg) these relative small test aircraft are representative for the main portion of the general aviation fleet in many countries[3].
Climb performance during initial climb-out after lift-off affects the noise impact in the surroundings of airports. For one of the test aircraft, the influence of take-off weight and of airframe drag reduction on observed noise levels is indicated. Also the effect of power reduction after lift-off is estimated.
Finally, test results are compared with predicted results of the existing emperical propeller noise estimating method developed by Hamilton Standard.

II. Measurement techniques and instrumentation

The measurements are performed at the general aviation airport Midden-Zeeland in the south-western part of the Netherlands, with low ambient background noise levels.
Windgradients, gusts, inversion and turbulence can have marked effects on the propagation of sound waves through the atmosphere, whereas analytical correction procedures for these phenomena are unreliable or do not exist at all.
Therefore the measurements are carried out under specific weather conditions. One of the requirements is a low windspeed, preferably below 3 m/s at 2 metres above ground level.
Unnecessary to mention that such conditions are quite rare in our (low) country.

Acoustic data.

To obtain the desired acoustic data, continuous tape recordings are made of the sound generated by the test aircraft during level and climbing flyovers at constant airspeed and power setting. In all cases the wingflaps were retracted. The geometry of the flight path, relative to measuring equipment is outlined in Figure 2.

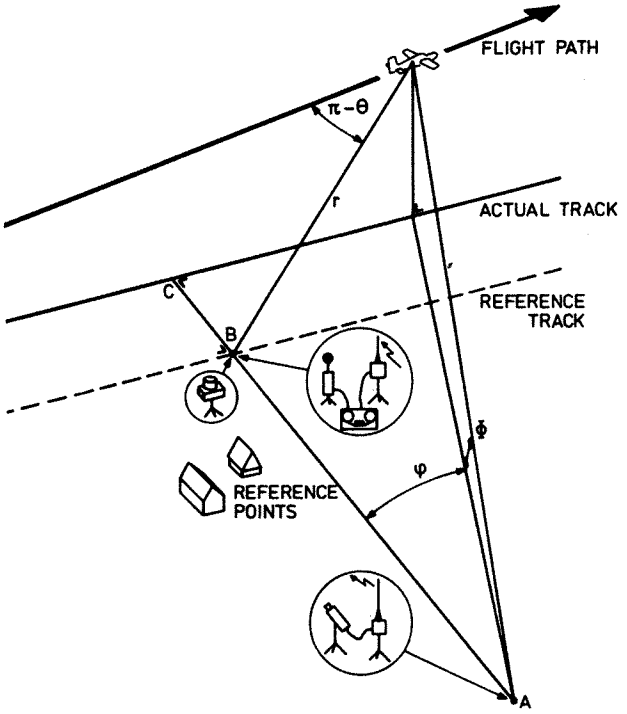

FIGURE 2. FLIGHT PATH GEOMETRY.

A free Field type condensor microphone is located in point B on top of a Brüel & Kjaer 2204 precision sound level meter. Its membrane is in horizontal position at 1.2 meter above the ground. The terrain surface consists of short-cut grass; no obstructions are present in the vicinity of the microphone. Via the sound level meter, acting as a pre-amplifier, the signal is fed unfiltered-except for frequencies under 20 Hz which are suppressed - into a Kudelski Nagra IV-D tape-recorder adapted for

acoustic measurements. The entire acoustic chain is calibrated by means of a sound level calibrator producing a 1000 Hz tone at 93.6 dB sound pressure level.
Frequency calibration is obtained by recording an electrical signal of constant amplitude and varying frequency (1 Hz-20 kHz).
Background noise is registered between fly-overs.

Flight path data

For conversion of measured sound data to reference conditions, the position of the aircraft relative to the microphone must be known at any moment during fly-over.
For this purpose flight path data are obtained by two photo-cameras[4]. One, an automatic Hasselblad, is located in point A of Figure 2.
It takes pictures from aside of the passing aircraft at one second intervals. Each time the shutter opens, the transmitter in A activates the receiver in B, which in turn feeds a 10 kHz pulse into the tape recorder, thereby synchronizing sound recordings with pictures.
The geometry of the test range was carefully laid out by the Department of Geodesy of Delft University. Hence, amongst other things, the distance AB between this camera and the reference track is known.
The reference track is marked by brightly colored cones. It is, however, not always possible for the pilot to see these cones clearly, especially in the nose-high attitude during climbing flights. Therefore actual and reference track will not always coincide. The distance BC between them, is measured by taking one picture with the second camera, located in B, when the aircraft passes the vertical plane through BC. The optical axis of this camera is directed vertically upwards.

Atmospheric conditions at 2 m height are determined with the aid of a hot-wire thermo-anemometer, a barometer and a hygrometer.

III. Data reduction

The recorded fly-over and background noise is analysed by means of 1/3-octave band (terts) filters using a B & K 2113 Audio Frequency Spectrometer and a B & K 2305 Level Recorder. The center frequencies of the filters are those recommended by IEC[5].
One thus obtains the sound pressure level in each terts band as a function of time.
By combining the results of the two cameras and the 10 kHz pulses on the sound recording, the angles φ, ϕ and distance AC in Figure 2 are known as a function of time.
From these data, altitude, distance r between aircraft and microphone and emission angle θ are deduced.
As a result every point on the sound time-history corresponds to a known value for r and θ.
Taking into account background noise level, distance r, atmospheric attenuation and speed of sound, ground attenuation where appropriate and microphone directional properties, the sound pressure level at a reference distance of 1 metre from the source as a function of emission angle (θ) in each terts-band (i) is determined. This is denoted as $L_{p_1}(\theta,i)$.
Assuming rotational symmetry about the aircraft longitudinal axis, the acoustic power in each terts band in terms of power watt level, PWL (i) is then calculated. The overall power watt level, PWL is obtained by logarithmic summation of the contributions of all terts bands. To describe the directional properties of the aircraft's sound radiation, the socalled Directivity Index DI (θ,i) is used. This is the difference between $L_{p_1}(\theta,i)$ and the sound pressure level at unity distance caused by a hypothetical sound monopole radiating the same acoustic power as the aircraft.
A brief description of the mathematical process of this data reduction is presented in Reference 7.
The advantage of this method is that it results in a set of basic noise quantities-PWL (i) and DI (θ,i)- from which sound pressure levels, peak noise levels as well as footprints and time histories in dB(A), dB(D), PNdB etc. can be derived in any point relative to the flight path. A few examples of this are presented in section V and VI of this paper.

IV. Test aircraft information

Principal dimensions and performance specifications of the test aircraft can be found in Figure 3. The engine performance is presented in Figure 4.

Type	Cessna 172	Cherokee
gross weight	1044 kg	975 kg
empty weight	565 kg	568 kg
span	10.9 m	9.1 m
length	8.2 m	7.1 m
height	2.7 m	2.2 m
wing area	16.2 m^2	14.9 m^2
aspect ratio	7.4	5.6
propeller diameter	1.93 m	1.83 m
max. rate of climb at sea level	3.3 m/s	3.3 m/s
speed for maximum rate of climb	132 km/h	137 km/h
max. speed at sea level	224 km/h	224 km/h

FIGURE 3. CHARACTERISTIC DATA OF TEST AIRCRAFT.

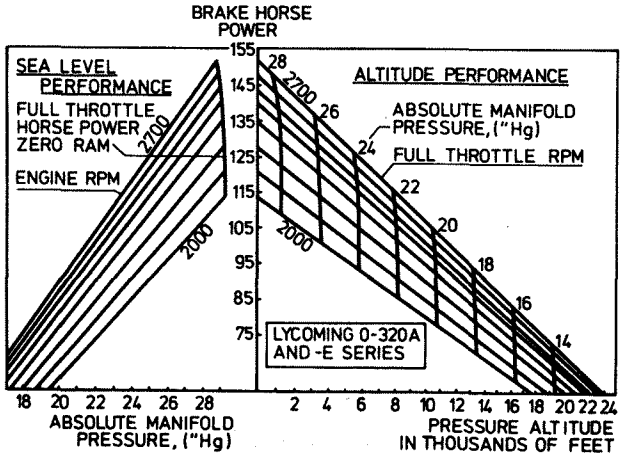

FIGURE 4. ENGINE PERFORMANCE.

Based on manufacturers performance data and drag calculations, performance diagrams- available and required horse power versus airspeed - were constructed. As an example, the result for the Cessna 172 is given in Figure 5. For this airplane the drag polar was taken from literature[6].

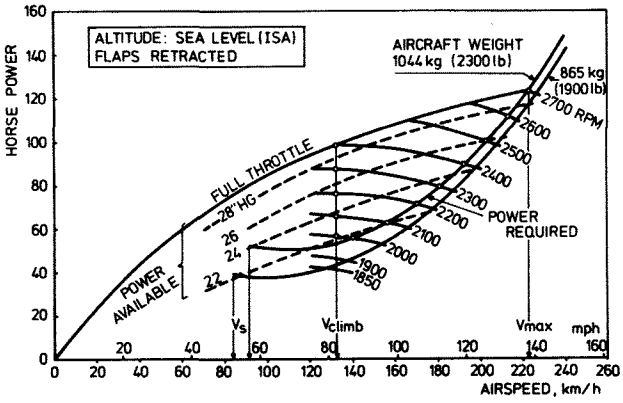

FIGURE 5. PERFORMANCE DIAGRAM FOR CESSNA 172 AIRCRAFT (ESTIMATED).

Figure 6 shows performance data - derived from Figure 5 - that are of interest for this investigation. Since none of the test aircraft is equipped with an inlet manifold pressure meter, engine brake horse power is only know at full throttle conditions. Therefore in particular the engine performance data in Figure 6 must be considered as an approximation.

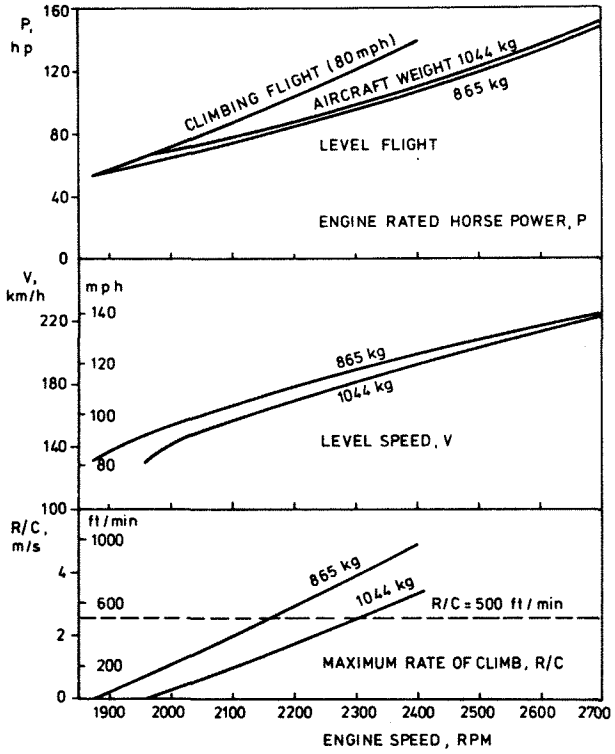

FIGURE 6. ENGINE AND AIRCRAFT PERFORMANCE CESSNA 172 AT SEA LEVEL (ESTIMATED).

V. Test results

Detailed measurement results of the Delft University test are presented in the references at the end of this paper[7-13]. Some results are presented in the following, they were all obtained using a comprehensive summary of all results obtained so far, that will become available soon[14].

Acoustic power

Values of overall acoustic power in terms of power watt level as a function of engine speed are presented in Figure 7 for both level and climbing flight. As could be expected, PWL increases with increasing engine speed.
At the same engine speed, more acoustic power is radiated in climbing flight than in level flight, since brake horsepower is higher (see Figure 6).

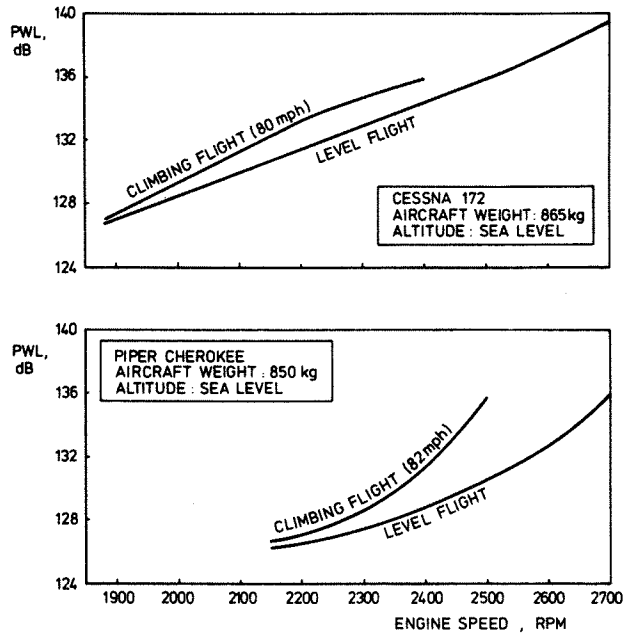

FIGURE 7. OVERALL POWER WATT LEVEL.

The distribution of the overall power watt level value over the 1/3-octave bands is presented in Figure 8 and 9 for level and climbing flights respectively. To make these spectra independent of the values of overall power watt level, the relative power watt level is plotted in Figure 8 and 9. This is denoted as ΔPWL(i) and defined by:

$$\Delta PWL\ (i) = PWL\ (i) - PWL$$

This quantity has a direct relation to the acoustic power ratio W(i)/W according to:

$$\Delta PWL\ (i) = 10 \log W(i)/W$$

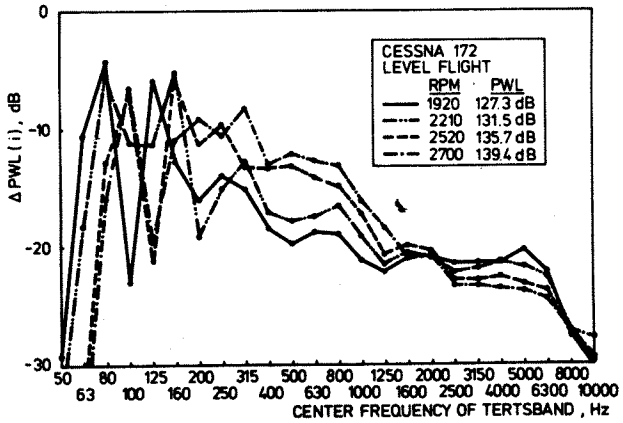

FIGURE 8. POWER WATT LEVEL SPECTRA

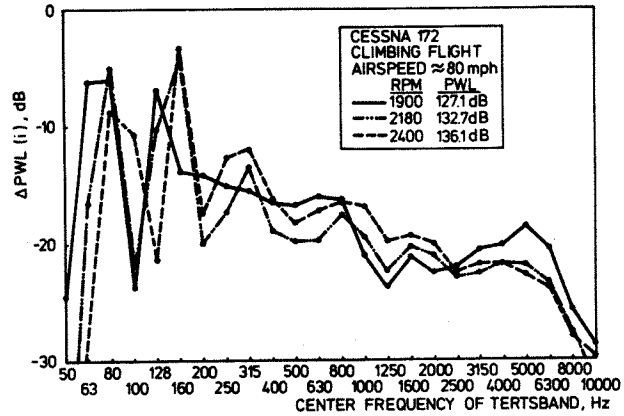

FIGURE 9. POWER WATT LEVEL SPECTRA.

From these Figures it appears that the contribution to overall acoustic power of the tertsband containing the blade passage frequency - for two bladed propellers equal to RPM/30 - is in almost all flight conditions of less importance than that of the tertsband containing the second harmonic, i.e. two times the blade passage frequency. Furthermore, the contribution of the third harmonic becomes more important as engine speed increases. Usually, experimental data for propellers are obtained from static ground tests, which show frequency spectra where the contributions of the low frequency rotational tone noises decrease with increasing harmonic number.
Though no conclusive explanation is as yet available, this shift, of the dominant frequency to higher harmonics probably is caused by the effect of for-

ward speed on harmonic content, as was found by other investigators when noise spectra were measured during both static and flyover operation[15].

Directionality

To get an impression of the directional properties of the acoustic power radiated by the test airplanes, Figure 10 is presented. Here for two different engine speeds in climbing flight, the overall Directivity Index, DI (θ) is given.

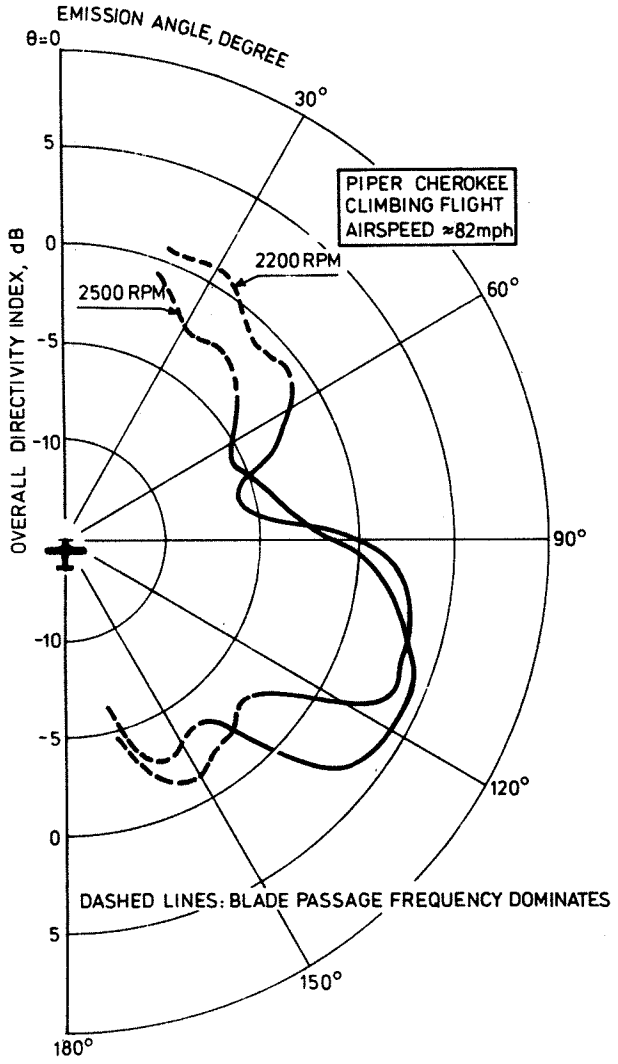

FIGURE 10. DIRECTIONAL PATTERN OF NOISE FIELD

Similar graphs can be constructed for the Directivity Index, DI (θ,i) for each 1/3-octave band of frequency[11]. The plots presented there illustrate the variation of the directivity pattern with frequency.

Sound pressure level

At given atmospheric conditions (atmospheric attenuation) the sound pressure level in a certain point is a function of the power watt level of the source, the distance from the source and the emission angle. To compare the different sound fields the sound pressure level at a reference distance may be used. Throughout this paper a reference distance of 1 metre is used, which sound pressure level is denoted as $L_{p_1}(\theta)$.

Figure 11 shows the effect of engine speed on the overall sound pressure level at reference distance in the direction of maximum overall Directivity Index.

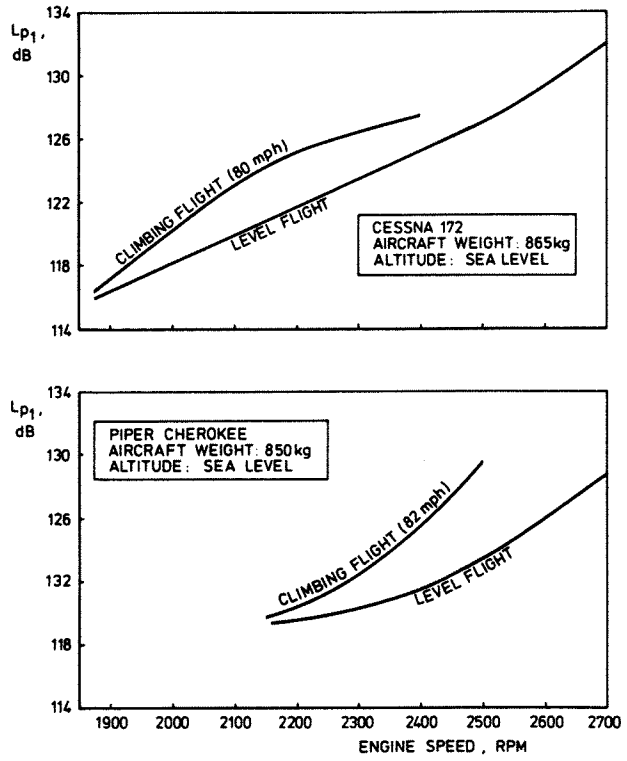

FIGURE 11. MAXIMUM SOUND PRESSURE LEVEL AT REFERENCE DISTANCE.

Concerning the frequency distribution of the sound pressure level, analysis of the test results revealed that the second harmonic is dominant for emission angles around the propeller plane. Only for very large and very small emission angles the blade passage frequency is more intense than the

second harmonic, as indicated by dashed lines in Figure 10.

To illustrate this further, the contribution of each 1/3-octave band to the overall sound pressure level L_{p_1} is presented in Figure 12 for two emission angles. Similar to the Figures 8 and 9, these spectra are plotted in terms of the sound pressure level at unity distance relative to the overall sound pressure level at unity distance relative to the overall sound pressure level, $\Delta L_{p_1}(\theta,i) = L_{p_1}(\theta,i) - L_{p_1}(\theta)$, which quantity is a measure for the sound intensity ratio $I(\theta,i)/I(\theta)$.

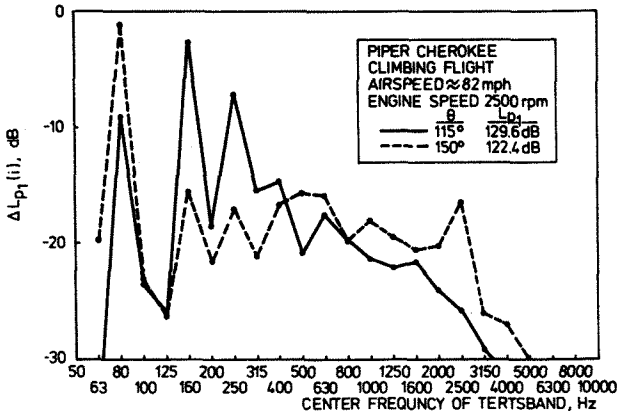

FIGURE 12. EFFECT OF EMISSION ANGLE OF NOISE LEVEL.

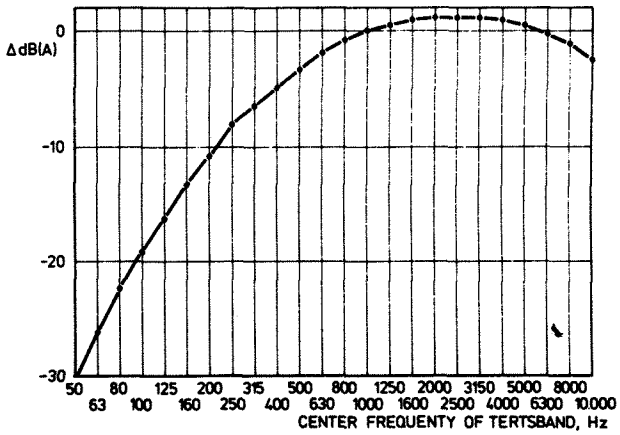

FIGURE 13. A-WEIGHTING FOR TERTSBAND FREQUENCIES.

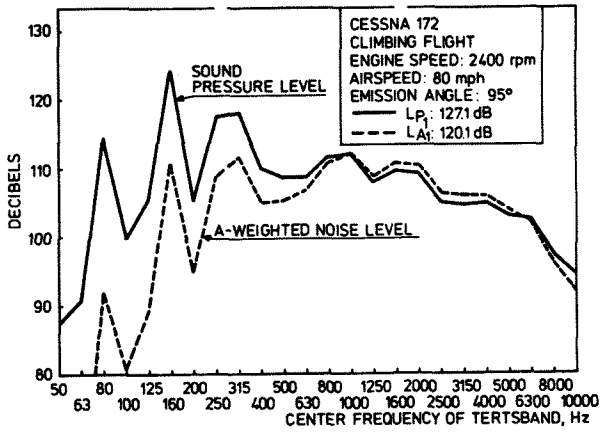

FIGURE 14. COMPARISON OF L_p AND L_A SPECTRUM AT REFERENCE DISTANCE.

A-weighted noise level

The A-weighted noise level, L_A, is used for certification purposes of light aircraft as well as for many other sources of industrial and traffic noise. It takes into account the human perception of noise, mainly by attenuating the contribution of the lower frequencies to the overall sound pressure level. The A-weighted noise level is obtained from the sound pressure level spectrum by adding a certain value, ΔdB(A) to the sound pressure level in each terts band (Figure 13).

To illustrate the effect of this weighting, both the sound pressure level and the A-weighted spectrum for the same flight condition are shown in Figure 14.

Contours of equal A-weighted noise level around the airplane are presented in Figure 15. These contours are adjusted for reference atmospheric conditions (sea level pressure of 76 cm mercury, ambient temperature 15°C, relative humidity of 70 percent, zero wind).

Typical for all test aircraft is that the emission angle where L_A shows a maximum, lies between 90° and 120°. One reason for this is the relative importance of the second harmonic frequency for these angles.

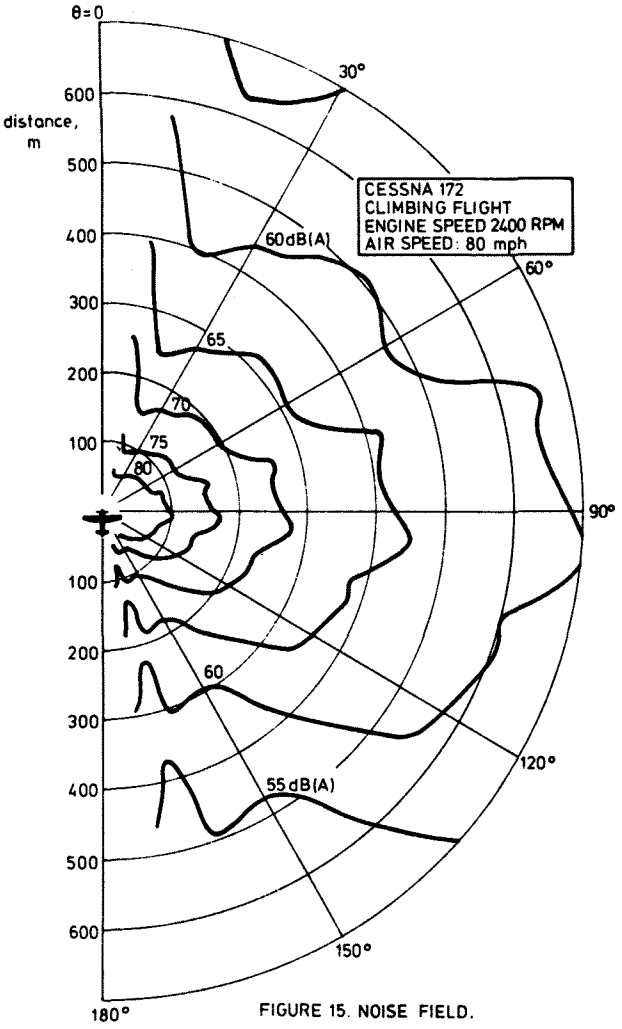

FIGURE 15. NOISE FIELD.

VI. Observed noise levels on the ground

Flyover noise

For a given flight condition, the relationship between maximum observed noise level in dB(A) and distance from the flight path can be obtained from graphs like Figure 15. To illustrate this, Figure 16 and 17 are presented. They are valid for the reference atmospheric conditions mentioned before. Figure 16 shows the maximum observed noise levels for the two test aircraft during steady state level flight for a number of engine speeds. Clearly, the airspeed varies with engine RPM. In Figure 17 the maximum noise levels on the ground during climbing flight are presented. Here the airspeed was held constant at about 80-85 mph, typical for climbing flights after lift-off with these aircraft.

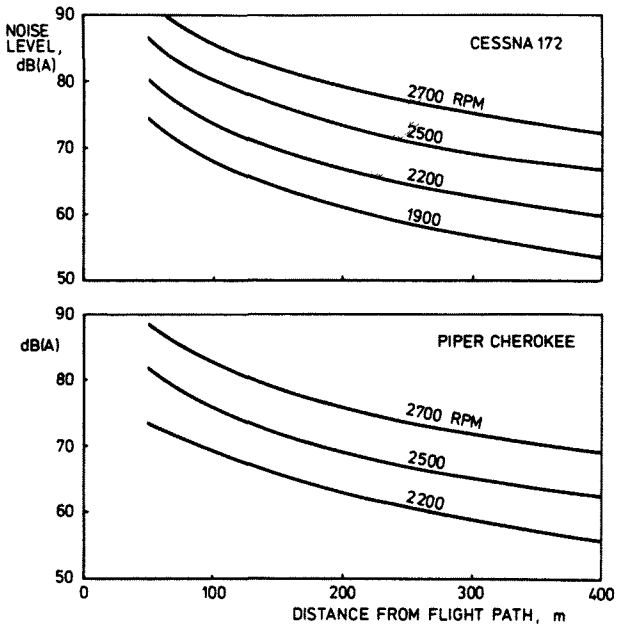

FIGURE 16. MAXIMUM OBSERVED NOISE LEVEL DURING LEVEL FLYOVER.

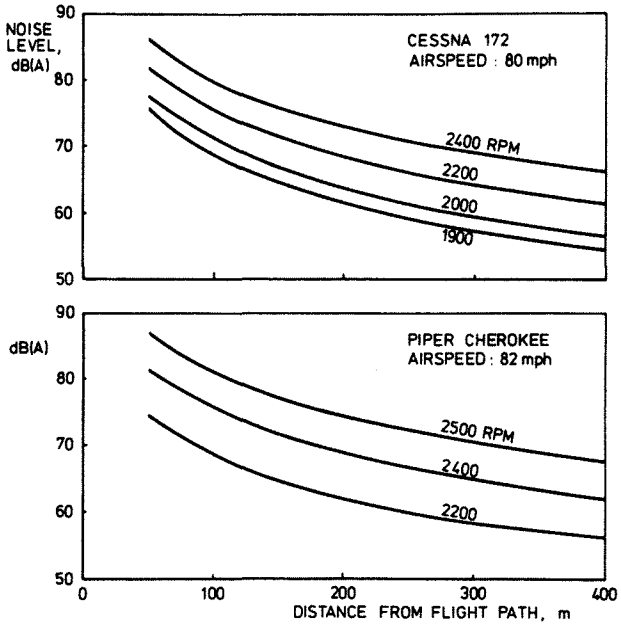

FIGURE 17. MAXIMUM OBSERVED NOISE LEVEL DURING CLIMBING FLYOVER.

An impression of the noise impact during climb-out can be obtained by using noise footprints, i.e. the contours of given peak noise level on the ground.

Using noise data from Figure 17 and performance data from Figure 6, examples of footprints are given in Figure 18.

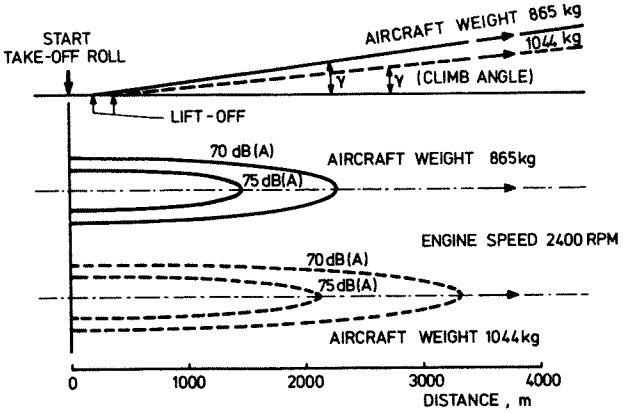

FIGURE 18. NOISE FOOTPRINTS FOR CESSNA 172.

Effect of aircraft weight

As can be concluded from Figure 18, aircraft weight affects take-off performance and thus the noise situation around airports. Figure 19 presents the effect of the test airplane's weight on noise levels during take-off under normal operational conditions.

Taken into account were the influence of weight on take-off run on a hard surface runway at constant lift-off speed and on climb performance at constant "handbook" power setting and airspeed. The upper part of Figure 19 shows the relative noise level in a point on the ground under the flight path at 2500 m from the start of the take-off run. In lower half, the effect on the 75 dB(A) footprint area measured from start of take-off run is given. Both curves are representative for both test airplanes. Since powersetting is the same for all weights, the width of the footprint at lift-off is constant. Therefore the footprint area is a measure for its length.

For these kind of airplanes an average passenger weighs about 9 percent of the gross weight. This means that one passenger is "worth" about 2 dB(A) and 20 percent footprint area. By the same reasoning, every 10 gallons of fuel is worth about 1 dB(A) and 8 percent footprint area.

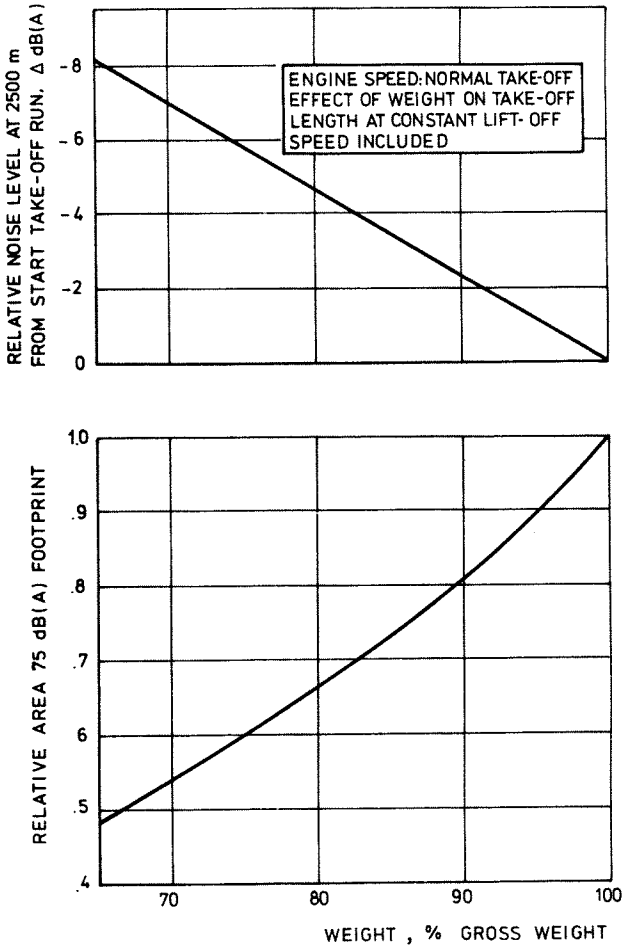

FIGURE 19. EFFECT OF AIRCRAFT WEIGHT ON NOISE LEVELS DURING TAKE-OFF.

Effect of power reduction

One way to diminish the noise levels on the ground in the vicinity of airports may be a decrease of engine speed after lift-off.

The effect of this is two fold. On the one hand the noise level at a given distance from the flight path decreases (see Figure 17), on the other hand the climb angle decreases causing a decrement of the distance from ground to airplane.

The net effect in terms of relative footprint area may be positive, as is shown in the upper part of Figure 20.

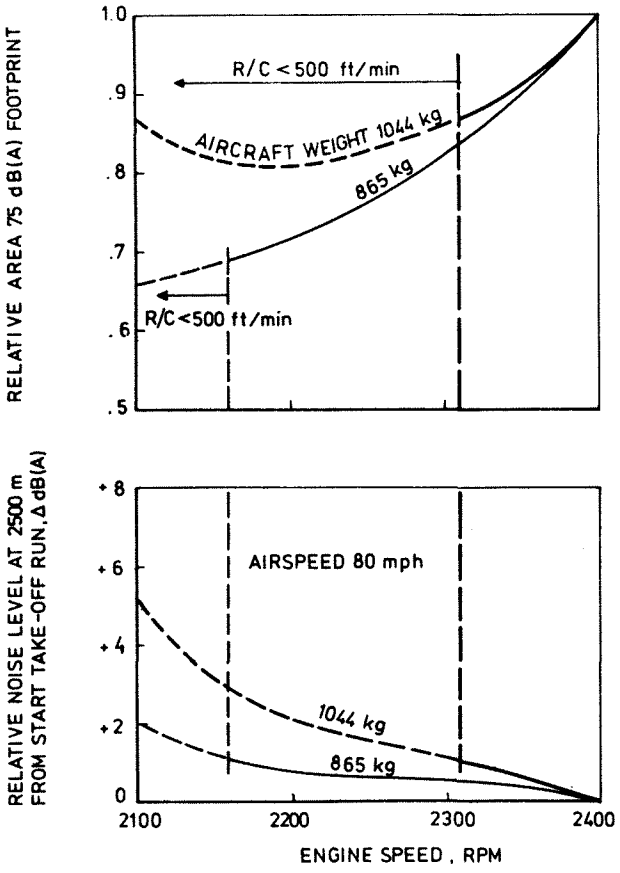

FIGURE 20. EFFECT OF ENGINE SPEED REDUCTION AFTER LIFT-OFF ON NOISE LEVELS DURING TAKE-OFF FOR CESSNA 172

Unfortunately the application of this measure is strongly restricted by flight safety considerations, when a rate of climb of 500 ft/min (2.54 m/s) is taken as a minimum (FAR 23 requirements). Since the width of the footprint just after lift-off diminishes with power reduction, the footprint area is no longer a measure for its length. It is therefore meaningful to observe the noise situation at given distance from the start of the take-off run. The results of this are presented in the lower part of Figure 20. Now the net effect is negative for the Cessna 172. From calculations for the Cherokee aircraft a positive result appears, however. Apparently, a general statement for this behaviour can not be made.

VII. Designing for noise control

The foregoing examples indicate that at given noise radiation (power setting), a steeper climb will lead to an alleviation of the noise impact on the ground. Figure 21 shows for one of the test aircraft to what extend climb angle improvement affects noise footprint area and noise level at given distance from start of take-off roll. Among other things, this Figure indicates that to obtain a reduction of 5 dB(A), a perceptible drop in noise level, an increment in climb angle of about three degrees is required.

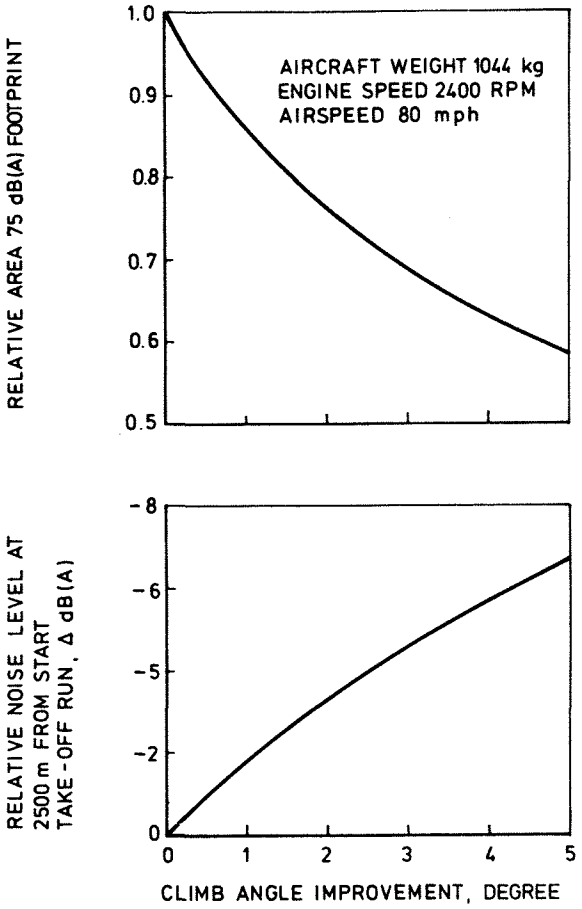

FIGURE 21. EFFECT OF CLIMB ANGLE ON NOISE LEVELS DURING TAKE-OFF FOR CESSNA 172

Climb performance depends on excess power available (propeller thrust x airspeed) over power required (aircraft drag x airspeed).

Apart from improving the engine-propeller performance, steeper climb angles can be obtained by drag reduction. To increase the climb angle by the three degrees mentioned earlier, the drag

coefficient must be about halved, assuming no change in airspeed. This will be difficult to realize, even by a drastic re-design of the airplane.
It seems therefore better to concentrate on reducing propeller and engine exhaust noise radiation, being the main sources of external noise.

For the development of optimized propellers and exhaust mufflers from noise, weight and performance standpoint, one needs at least well reflecting engineering methods to predict the properties of these aircraft components.
Although the engine does contribute to aircraft noise, in general, propeller noise is dominating for the aircraft types considered here[16]. In view of this some attention is paid to an existing noise calculation procedure for small diameter propellers.

VIII. Noise prediction method of Hamilton Standard

Besides theoretical calculation procedures an emperical method is available for general aviation propellers, developed by Hamilton Standard[17]. According to this publication, the method is based mainly on a number of tests. Due to its relative simplicity and ease of use, it can be a suitable tool for sensitivity studies on propeller geometrics. As an example, this method will be applied to the Cessna 172; the results will be compared with those of noise measurements described earlier in this paper.
The noise estimation method of Hamilton Standard enables the calculation of the maximum observed noise level at a given distance from the source. Details of blade shape are not considered in this method, input is limited to the following design and operational parameters:

- Propeller diameter, D.
- Number of blades, B.
- Propeller speed, n.
- Engine shaft-brake horse power, P.
- Airspeed, V.
- Speed of sound, a.
- Distance, relative to the propeller(s), to the point where the noise level is to be calculated, R.

From various graphs presented by Hamilton Standard, the following relationship between these parameters and the maximum sound pressure level at distance R is established:

$$L_{p_R} = 80.5 + 15.3 \log P - 20 \log D + 38.5 M_t - 3(B-2) - 20 \log R$$

where

$M_t = \pi nD/a$, propeller rotational tip Mach number.
Both D and R are expressed in metres.
Clearly, atmospheric attenuation of sound, which is proportional to distance and a function of temperature, relative humidity and sound frequency, is not considered.
Recently, this equation was somewhat modified by

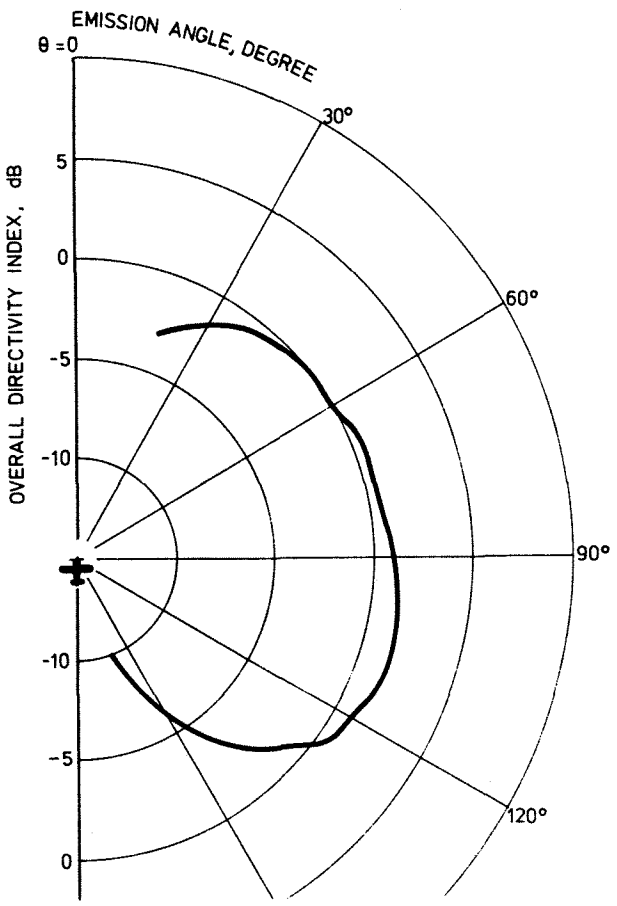

FIGURE 22 DIRECTIVITY INDEX.

Swiss researchers, based on results of certification tests on small propeller driven aircraft[18]:

$$L_{p_R} = 76.1 + 16 \log P - 20 \log D + 38 M_t - 3(B-2) - 20 \log R$$

The predicted maximum sound pressure level will occur at an emission angle θ of approximately 105°, according to the directionality defined in Reference 17, from which Figure 22 is derived. The method assumes the directional properties to be independent of aircraft type and the aircraft flight and engine condition.
The test data reveal a more pronounced sound radiation-higher values for DI- in a range of emission angles between 85 - 120° (eg. see Figure 10).

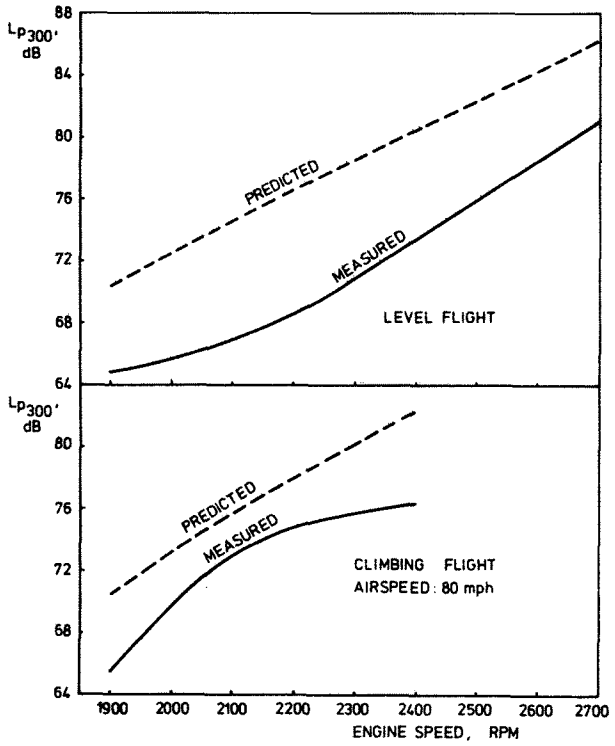

FIGURE 23. MEASURED AND PREDICTED SOUND PRESSURE LEVELS AT A DISTANCE OF 300m FOR CESSNA 172.

In Figure 23, predicted and measured maximum sound pressure levels versus engine speed at a distance of 300 m are plotted for the example airplane.
The predicted values are calculated by means of the latter, modified, equation and are based on horse power data from Figure 6. In spite of the more uniform sound radiation, this Figure shows that the prediction method over-estimates the sound pressure level in both flight conditions.

For the calculation of the A-weighted noise level, L_A, knowledge of the frequency spectrum is needed. Figure 24 shows the predicted spectra as a function of rotational propeller harmonic and helical tip Mach number, M_{t_v} $(= \sqrt{V^2+(\pi nD)^2}/a)$.

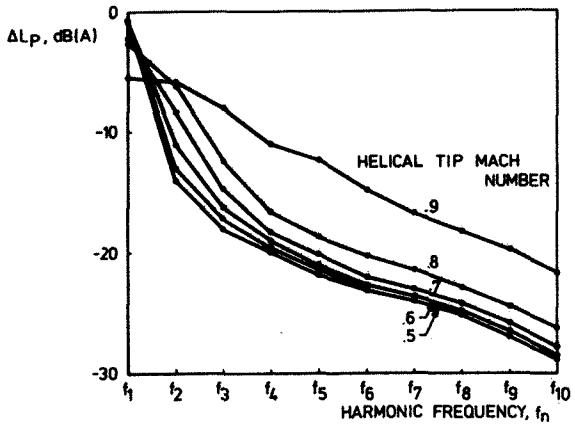

FIGURE 24. SOUND PRESSURE LEVEL SPECTRA ASSUMED IN PREDICTION METHOD OF HAMILTON STANDARD.

Comparison of Figure 24 with Figure 12, where $M_{t_v} = 0.71$, indicates that the shape of the predicted frequency spectrum clearly differs from the measured spectra. Furthermore, the assumption in Figure 24 that the sound emission only occurs at series of tone noises, is not in accordance with the measurement results.
To some extent, the differences are probably caused by the fact that the noise data on which the prediction method is based, were obtained from static tests[19] (V = 0).
The under-estimation of the relative importance of the second and higher harmonics results in an underestimation of the A-weighted noise level.
The two errors introduced by this method, over-estimating the sound pressure level and under estimating L_A for a given value of the sound pressure level, tend to cancel each other. As a result, the predicted values for L_A are more or less comparable with test results, indicated by Figure 25.

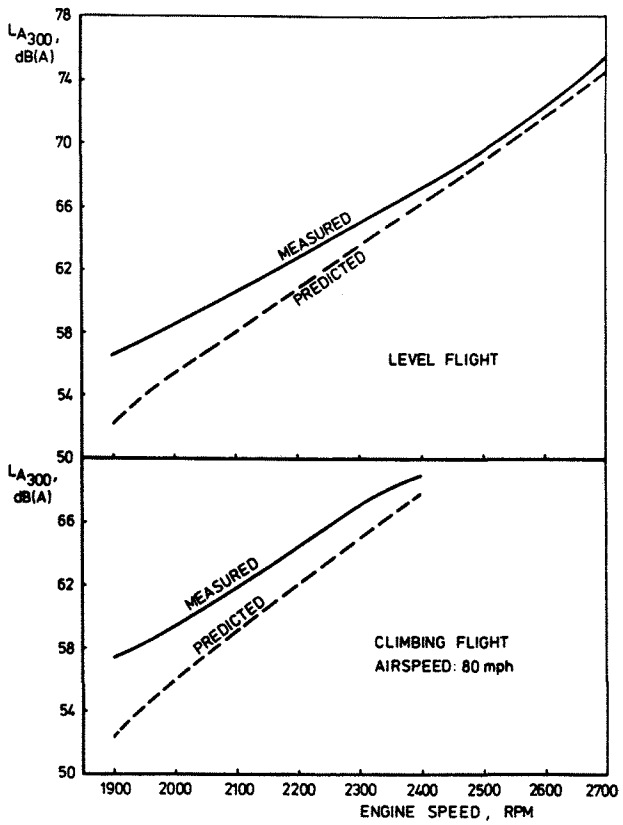

FIGURE 25. MEASURED AND PREDICTED NOISE LEVELS AT A DISTANCE OF 300 m FOR CESSNA 172.

IX. Concluding remarks

The authors of this paper feel that a really effective noise reduction of propeller-driven light airplanes can only be achieved by concentrating on diminishing the noise at the source, that is of the propeller-engine combination.

The optimization of propellers for minimum noise while maintaining an adequate performance level requires knowledge of the effect of propeller shape and size parameters on both noise production and on propeller thrust in the presence of other parts of the aircraft.

Also the contribution of the engine itself to the total noise level has to be studied.

To this end, more experimental and theoretical research is needed.

The authors were therefore happy to learn that for instance, the Department of Aerospace Engineering of the University of Kansas in Lawrence, through a NASA grant, will also perform further external (and internal) noise measurements on small general aviation airplanes. This program will be performed in cooperation with and based on the know-how and experience gained by the Department of Aerospace Engineering of Delft University.

The development of accurate engineering methods to predict noise levels of these aircraft, a prerequisite to the design of quiet light airplanes, is one of the goals of the programs of both universities.

References

1. Federal Aviation Regulation, Part 36, Appendix Noise Requirements for Propeller-Driven-Small Airplanes, 1975, FAA, Department of Transportation, Washington, D.C.

2. Committee on aircraft noise; International Civil Aviation Organization, third meeting, Montreal 5-23 March 1973, Doc 9063, CAN 3.

3. Some data on general aviation aircraft in Europe, ITA Bulletin No 35/21 October 1974.

4. Th. van Holten, P. Kapteyn, G.J.J. Ruijgrok and C. Vermeulen, Description of a photographically determination of the flight path, Delft University of Technology, Department of Aero-Space Engineering, Memorandum M-206, 1973 (in Dutch).

5. ISO Recommendation R 226: Preferred frequencies for acoustical measurements, August 1962.

6. J. Latas, Aerodynamic Development of the Cessna 177, SAE Paper 680199.

7. G.J.J. Ruijgrok, Measurements of external noise from light propeller-driven aircraft, Delft Progress Report, Series C, Vol. 1, Sept. 1975, p. 84-92, Delft University of Technology, Netherlands.

8. Th. van Holten, P. Kapteyn and G.J.J. Ruijgrok, Sound measurements of the Piper Aircraft type PA-24-250 Comanche, Delft University of Technology, Department of Aerospace Engineering, Memorandum M-190, 1973 (in Dutch).

9. Th. van Holten, P. Kapteyn and G.J.J. Ruijgrok, Sound measurements of the Piper aircraft type PA-34 Seneca, Delft University of Technology Department of Aerospace Engineering, Memorandum M-217, 1974 (in Dutch).

10. Th. van Holten, P. Kapteyn and G.J.J. Ruijgrok, Sound measurements of the Piper aircraft type PA-28-R-200 Arrow, Delft University of Technology, Dept. of Aerospace Engineering, Memorandum M-218, 1974 (in Dutch).

11. Th. van Holten and G.J.J. Ruijgrok, Sound measurements of the Piper aircraft type PA-28--140 Cherokee, Delft University of Technology, Dept. of Aerospace Engineering, Memorandum M-230, 1975 (in Dutch).

12. F.W.J. van Deventer, G.J.J. Ruijgrok and C. Vermeulen, Results of noise measurements of the general aviation aircraft type Cessna F 172 M, Delft University of Technology, Dept. of Aerospace Engineering, Memorandum M-249, 1976.

13. F.W.J. van Deventer, G.J.J. Ruijgrok and C. Vermeulen, Results of noise measurements of the Piper PA-18-150 Super Cub, as banner towing aircraft, Delft University of Technology, Dept. of Aerospace Engineering (to be published).

14. Tabulated results of external noise measurements of light propeller driven aircraft during flyover (to be published).

15. F.W. Barry and B. Magliozzi, Noise Detectability prediction methods for low tip speed propellers, Air Force Flight Dynamics Lab., Technical Report AFFDL TR 71-37, 1971.

16. D.J. Maglieri and H.H. Hubbard, Factors affecting the noise from small propeller driven aircraft, SAE Paper 750516.

17. R. Worobel and M.G. Mayo, Advanced general aviation propeller study, NASA CR 114289, 1971.

18. G. Dübener, Fluglärmbekämfung bei Propellerflugzeugen, Aero-Reuve 12/1973, p. 628-630.

19. F.B. Metzger and B. Magliozzi, New directions in aircraft propulsor noise research, SAE Paper 750515.